Spatio-temporal Distributions of the Wind Stress and the Thermocline in the East Sea of Korea*

Jung-Yul NA and Sang-Kyu HAN
Department of Earth and Marine Sciences, Hanyang University, Kyung Gi Do 425-791, Korea

The wind stress distribution over the East Sea of Korea was obtained from the shipboard observations of the Fisheries Research and Development Agency along the serial observation lines. These monthly and annual mean wind stress distributions were put into the simplified interface model which describes the latitudinal variations of the upper-layer thickness as function of the curl of the wind stress.

The observed variations of the surface, zonally averaged winds indeed caused the upper-layer flow convergent and divergent at the latitudes that produced a zone of thick upper-layer or a deep permanent thermocline and the shallower depth with divergence. Thus, the wind field contributes positively to maintain the almost time-independent distribution of the interface of "saddle like" feature in north-south direction over the study area.

Introduction

According to the results of long term average of the depths of permanent thermocline in the East Sea of Korea (National Federation of Fisheries Cooperative, 1977) a pronounced spatial variation of the depths in north-south direction clealy exists throughout the year. Fig. 1 shows an example of such variations that could be described as "saddle-like" feature, i. e., two deepest parts exist along the longitudinal direction and the depth becomes shallower in the region near 37°N latitude.

If the depth of permanent thermocline corresponds to the thickness of upper layer, one can easily-deduce the pattern of the surface currents via geostrophic relationship. However, the pattern will not reveal the observation flow fields in that two branches of the Tsushima Current, among them, one flows northward along the Korean coast as the East Korea Warm Current (EKWC) and the other flows along the Japaness coast.

Unfortunately the spatial distribution of permanent thermocline analyzed covers only the region close to the eastern coastal area of Korea, but no such pronounced north-south varitions of the depth of thermocline have been observed elsewhere.

The region considered here includes most of the dynamically significant features such as the East Korea Warm Current and its separation from the coast. Moreover it is under most sensitive influence by the seasonal fluctuations of the Tsushima Current which is known to be the strongest during late summer (Lee and Whang, 1981 ; Mitta and Ogawa, 1984). However the monthly distribution of the depth of permanent thermocline shows independent behavior regardless of strong seasonal variations of thermal properties of the upper layer (Kang, 1985). Branching of the Tsushima Current (Byun and Chang, 1984. Yoon, 1982) and the seasonal fluctuations in volume transport (Yi, 1966) may influence the spatial pattern of the thermocline depth.

The lack of avaiable wind data over the East Sea of Korea and the dominant role of the Tsushima Current in the dynamics of the current systems in

*이 논문은 1987년도 문교부 기초과학 연구비에 의하여 연구되었음.
부산수산대학 해양과학연구소 연구업적 제209호

the sea may have hindered anyone from seeing an independent effect of wind on the dynamics of some isolated phenomena. The wind-driven influence on the branching of the Tsushima Current in terms of the seasonal variations of wind stress was investigated numerically (Sekine, 1987), however, the winter season with negative wind stress curl and the weak wind stress with positive wind stress curl during the summer season did not produce the spatial feature of the thermocline in our study area. In the study area the deepest northern part may coincides, roughly, with the region of EKWC's separation from the coast (Hong and Cho, 1983), but the rest does not represent any observational pattern.

Bases on the almost time-independent existence of the interface between the seasonally varying upper-layer and the nearly quiescent low layer the influence of annual variations in atmospheric conditions, namely the wind stress, on the maintenance of the interface should be examined. It implies that wind-driven flow may eventually accumulates upper layer water and produce uneven distribution of the thickness of the upper layer of different density.

Therefore the purpose of this paper is to find wind stress distribution over the study area and to look into whether the annual mean wind field contributes to maintenance of the interface. Furthermore the Tsushima Current and the Ekman transport or the resultant pressure gradient will be examined to identify the role of wind fields over the study area.

Interface model

Since we want to compare the results of the present calculation with observation, it is necessary to identify the permanent thermocline with some density surface. Therefore the density stratification is idealized in terms of two homogeneous layers. Assuming the vertical transfer of horizontal stress is the only modification to geostrophic-hydrostatic balance, the flow of the interior sea is determined by the following equations (Veronis, 1973) (in rectangular coordinates) :

$$-fv = -\frac{1}{\rho}\frac{\partial p}{\partial \chi} + \frac{\partial \tau x}{\partial z} \quad \cdots\cdots (1)$$

$$fu = -\frac{1}{\rho}\frac{\partial p}{\partial y} + \frac{\partial \tau y}{\partial z} \quad \cdots\cdots (2)$$

$$\frac{\partial p}{\partial z} = -\rho g \quad \cdots\cdots (3)$$

$$\frac{\partial u}{\partial \chi} + \frac{\partial v}{\partial y} + \frac{\partial w}{\partial z} = 0 \quad \cdots\cdots (4)$$

where x is positive eastward, y is positive northward, and z is positive upward : the corresponding velocity components are u, v, w ; eastward stress is denoted by τx and northward stress by τ_y ; $f=2\Omega\sin\phi$ is the Coriolis parameter.

For the two-layer system, let $z=h_2$ be the thermocline and $z=h_1$ be the top surface and $z=0$ be the level bottom. Then the thickness of the layer is given by

$$h=h_1-h_2 \quad (5)$$

The hydrostatic equation together with the assumption of constant atmospheric pressure gives the pressure gradients in the two layers in terms of the height variations as

$$\frac{1}{\rho_1}\nabla p_1 = g\nabla h_1 \quad \cdots\cdots (6)$$

$$\frac{1}{\rho_2}\nabla p_2 = g\left(\frac{\nabla\rho}{\rho_2}\nabla h_2 + \frac{\rho_1}{\rho_2}\nabla h_1\right) \cdots (7)$$

where $\Delta\rho$ is $\rho_2-\rho_1$ and ∇ corresponds to horizontal gradient.

Assuming a flow driven by a zonal wind stress only and no transfer of stress at the interface the boundary conditions at the top and the interface are

$$\tau x = \tau, \quad \tau y = 0 \quad \text{at} \quad z = h_1 \cdots\cdots (8)$$

$$\tau x = \tau y = 0 \quad \text{at} \quad z = h_2 \cdots\cdots (9)$$

respectively. τ is the zonally averaged zonal wind stress per unit mass.

Since there is no momentum transfer to the bottom layer except in those regions where upper-layer water is abscent, wherever upper-layer exists, the lower layer is quiescent. Thus from eq. (7)

$$\nabla h_2 = -\frac{\rho_1}{\nabla \rho} \nabla h_1 \quad \cdots\cdots (10)$$

and use of eq. (5) leads to

$$\nabla h_1 = \frac{\nabla \rho}{\rho_2} \nabla h \quad \cdots\cdots (11)$$

Vertical integration of equations (1) to (4) over the upper layer by use of equations (10) and (11) then yields the transport equations

$$-fV = -g^1 \frac{\partial}{\partial x}\left(\frac{h^2}{2}\right) + \tau \quad \cdots\cdots (12)$$

$$fU = -g^1 \frac{\partial}{\partial y}\left(\frac{h^2}{2}\right) \quad \cdots\cdots (13)$$

$$\frac{\partial U}{\partial x} + \frac{\partial V}{\partial y} = 0 \quad \cdots\cdots (14)$$

where

$$U = f\int_{h_2}^{h_1} u dz, \; V = f\int_{h_2}^{h_1} v dz \text{ and } g^1 \equiv g\frac{\Delta \rho}{\rho_2}$$

Cross differentiation of eq. (12) and eq. (13) and use of eq. (14) give.

$$\beta V = -\frac{\partial \tau}{\partial y} \quad \cdots\cdots (15)$$

which is the Sverdrup transport relation.

Equation (12) can now be solved for h^2 by substituting the value of V from eq. (15). Thus, we have

$$\frac{\partial}{\partial x}\left(\frac{h^2}{2}\right) = \frac{1}{g^1}\left[-\frac{f}{\beta}\frac{\partial \tau}{\partial y} + \tau\right] \quad \cdots\cdots (16)$$

and, since right-hand side is independent of x, we can integrate eq. (16) to obtain

$$h^2 = h_{x_0}^2 - \frac{2}{g^1}\left[-\frac{f}{\beta}\frac{\partial \tau}{\partial y} + \tau\right](x_0 - x) \quad \cdots\cdots (17)$$

where h_{x_0} is the value of h at $x = x_0$.

Eq. (17) yields some interesting information. The magnitude of the terms in the square bracket, which depends on the latitude, will produce a latitudiual variation of h, the thickness of upper layer. Once the value of $\frac{\partial \tau}{\partial y}$ is known at some latitude the east-west variations of h can be determined.

Temporal and spatial variations of the wind stress

Determination of the wind stress over the study area is not an easy task, for the dominance of synoptic fronts during winter and summer and the period of ship observations limited by severe weather. One possible way of overcomming the aforementioned limitation could be the geostrophic computations of wind data using atmospheric pressure data. However, if one needs to compute *latitudinal* variations of wind stress, the error arising from the interpolation of isobars could exceed the magnitude of variation of wind stress, especially for the present study area that is a part of Japan Sea.

Therefore, an effort will be concentrated to compute characteristic wind field out of the presently avaiable wind observations. Aside from the Japan Meteorological Agency (JMA) buoy No. 6 data (located 37°45'N, 134°23'E), two major historical wind data over the East Sea of Korea are available from : (a) serial ship observations by the Fisheries Reasearch and Development Agency (FRDA) and (b) coastal weather observations by the Centeral Meteorological Office (CMO). However, the wind data from the meteorological stations along the east coast of Korea may not be suitable for the calculation of sea surface wind stress due to their locations affected by local conditions such as an orography. For example, the most frequent wind at two different stations, Sokcho and Pohang, during the months of August and December has revealed that the wind at Sokcho is southeasterly and Pohang is north-northeasterly during the August, while westerly and west-southwesterly are the most frequent wind at Sokcho and Pohang respectively, for the month of December (Table 1 and 2). In order to calculate the wind stress over the open sea area the wind fields observed from the same area is necessary, but the data from Ulreung-do station is excluded because of incoherent wind directions (Table 3). As stated previousely the bi-monthly wind observations by FRDA were usually done during the fair weather conditions. To make these data representative the wind

Table 1. Three most frequent wind (Aug.) (1980~1985)

position	Freq. (%)	WD	WS(*m/sec*)
	17.2	SW	6.4*
Bouy 6	17.2	SSW	3.9
	10.8	S(E)	2.4
	9.3	SE	5.8
SOGCHO	8.8	ESE	5.7
	8.1	E	5.8
	14.6	NNE	7.8
POHANG	14.4	N	7.7
	13.8	WSW	6.0
	35.1	NE	7.7
ULREUNG DO	24.5	SSW	8.8
	9.6	SW	8.2

* : The strongest wind among the components (16).

Table 2. Three most frequent wind (Dec.) (1980~1985)

position	Freq. (%)	WD	WS(*m/sec*)
	11.7	W	7.6
Bouy 6	11.4	N	8.7
	11.2	WSW	8.1
	28.8	W	7.8*
SOGCHO	23.2	WNW	7.8
	10.0	WSW	6.7
	29.7	WSW	6.5
POHANG	19.9	W	6.7
	17.3	SW	7.0*
	16.1	SSW	8.9*
ULREUNG DO	16.0	NE	7.9
	13.8	SW	7.8

* : The strongest wind among the components(16).

Table 3. Winds at open sea and Ulreung Do stations

		wind direction		wind speed(*m/sec*)	
date	st. no.	FRDA	Ulreun Do	FRDA	Ulreung Do
80. 2. 22	105-09	NNE	S	10.2	8.3
. 22	10	E	S	10.2	8.3
. 18	11	SE	SSW	10.2	10.3
80. 2. 21	105-09	SW	NE	5.6	8.7
. 21	10	NW	NE	5.6	8.7
. 21	11	NW	NE	5.6	8.7
83. 2. 14	105-09	SW	SSW	5.6	13.7
. 14	10	NW	SSW	5.6	13.7
. 4	11	SW	SSW	5.6	9.7
84. 2. 12	105-09	NE	NNE	1.5	6.7
. 11	10	NE	SSW	3.4	7.3
. 11	11	NE	SSW	3.4	7.3
85. 2. 6	105-09	SW	SSW	3.4	6.3
. 6	10	SW	SSW	3.4	6.3
. 6	11	SW	SSW	3.4	6.3

data from the buoy No. 6, which were observed every three hours, were used as reference for both direction and speed (Table 4). Furthermore, the wind of short period of fluctuations in direction were excluded before taking zonal average.

The wind directions that were not steady during the observation were also excluded to obtain relatively uniform wind fields, and also the FRDA sta-

Table 4. Composition ofwind speeds by Beaufort scale at three locations

Month	Buoy #6	106-line	105-line
2	4	1	2
4	3	2	2
6	3	2	2
8	2	1	1
10	3	1	2
12	5	2	2

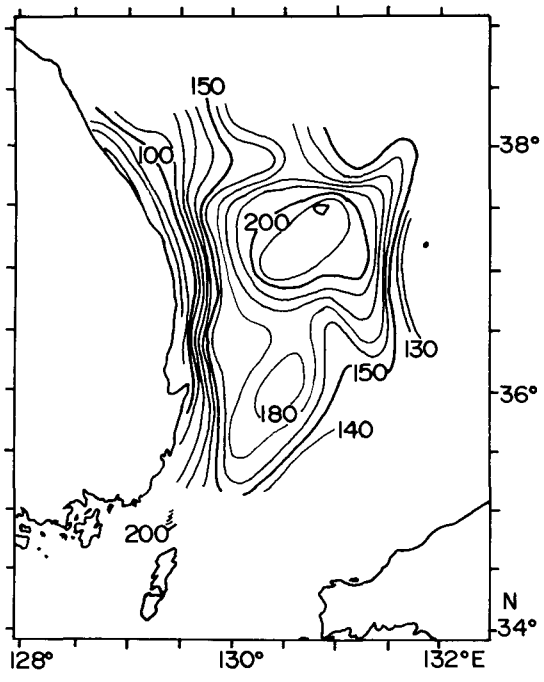

Fig. 1. Depth of permanent thermocline in December.

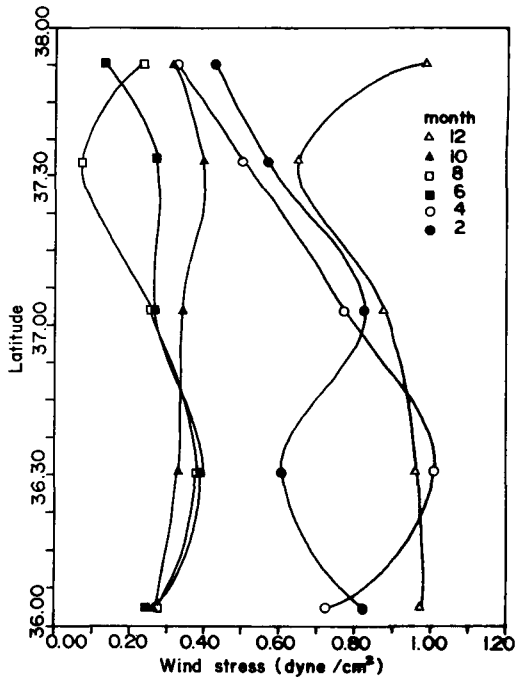

Fig. 3. Latitudinal variations of monthly averaged wind stress.

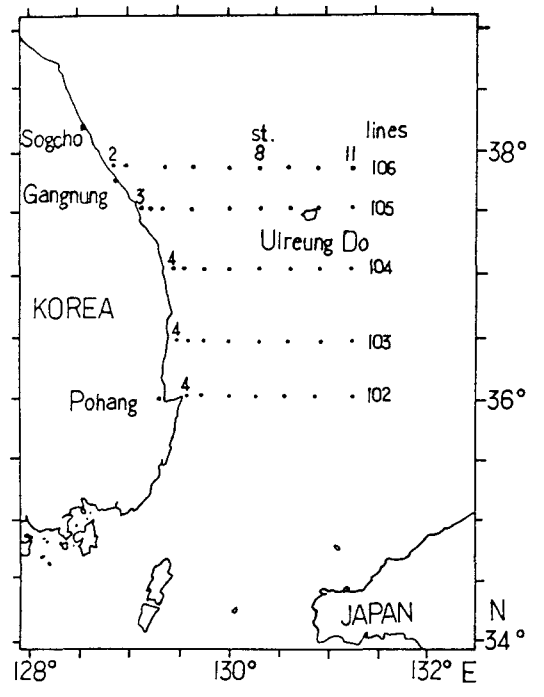

Fig. 2. The map of the FRDA serial line observations.

tions close to the coast were not taken into consideration for zonal average of the wind. Four stations (8 to 11 in Fig. 2) that are located relatively open sea were used to produce the latitudinal variations of wind stress. The wind speeds at each line were modified according to the winds at the buoy No. 6 such that the winds during the foul weather periods can be included for analysis.

The Figure 3 and 4 show the latitudinal variations of the zonally averaged zonal surface wind stress computed from 20 years (1965−1984) observations by FRDA. The values obtained from the observations are indicated by the symbols corresponding to the FRDA serial lines. The solid curve is obtained from a ploynomial curve whose coefficients are determined by minimizing the squared error from the observed points. The difference in wind stress magnitude is clearly seen for both north-south directions and seasonally, i.e., the stronger wind stress during the winter months.

In Figure 5 $\frac{\partial \tau}{\partial y}$ has been determined from derivatives of the approximating curve of the wind st-

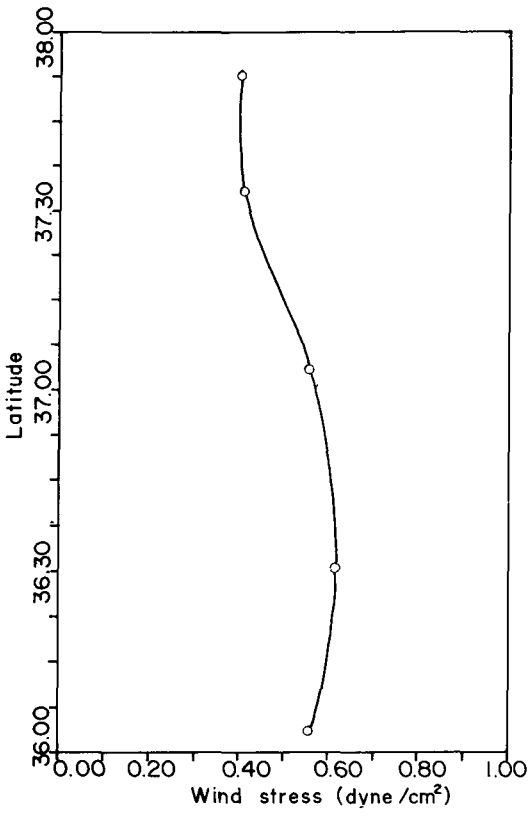

Fig. 4. Zonally averaged wind stress distribution ; yearly mean.

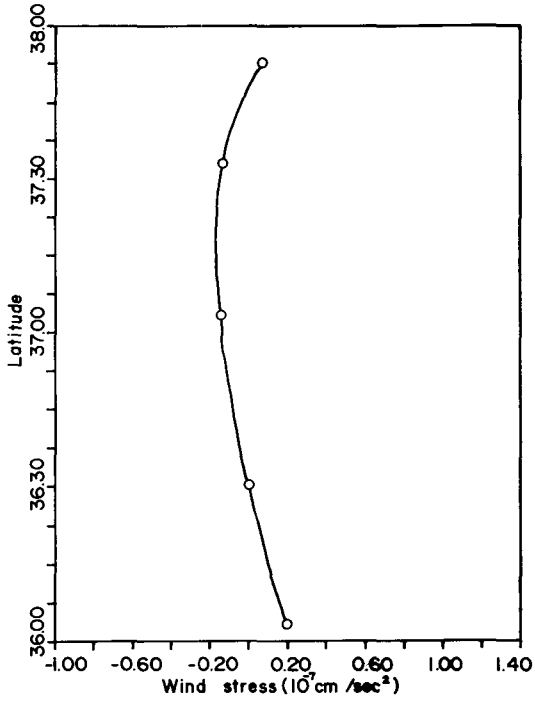

Fig. 5. Latitudinal variation of zonally averaged wind stress.

ress in the Figure 4, the yearly mean of the zonal wind stress. In fact it is the curl of wind stress since the meridional component of wind has been neglected. From the equation (15), the sign of $\frac{\partial \tau}{\partial y}$ determines the north-south flow so that convergence and divergence occur around 37°43'N and 36°30'N, respectively. This means that, in the two layer system, the thickness of the upper layer will be such that it becomes thick where the convergence occurs while it becomes thin where the divergence takes place.

The Figure 6 shows the north-south distribution of a normalized depth that has been determined by use of the equation (17). The open circles and the curve are obtained by the same procedure described for the wind stress.

The absolute magnitude of the thickness difference in the Figure 6, can be estimated by selecting a value of hx_0, the thickness at some longitude h. For example, if hx_0=200m, the difference will be 20 m which is far less for the northern sector but, at least qualitatively, is close to the value for the southern sector.

To see seasonal variations of the upper layer thickness, the summer and the winter seasons, corresponding to the months of August-October and February-April respectively, were chosen (Fig. 7). Since the present simplified two-homogeneous-layered model could be applied to a seasonal or the permanent thermocline as an interface, the depth (Fig. 7) can be compared with the one, corresponding to the months of April and October. A qualitative comparison shows an agreement, at least, in tendency of its north-south variations. It should be also noted that since the wind fields have been zonally averaged the same latitudinal variations of the depth must appears at any longitude. However, if any zonal variations of wind stress exist, the longitudinal variations of the depth should exist accordingly.

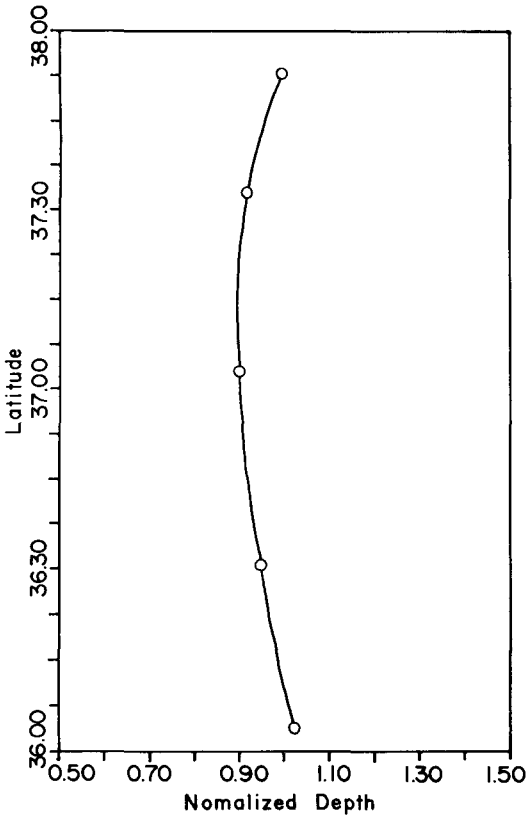

Fig. 6. The north-south variation of h^2/hx_0^2 in eq. (17).

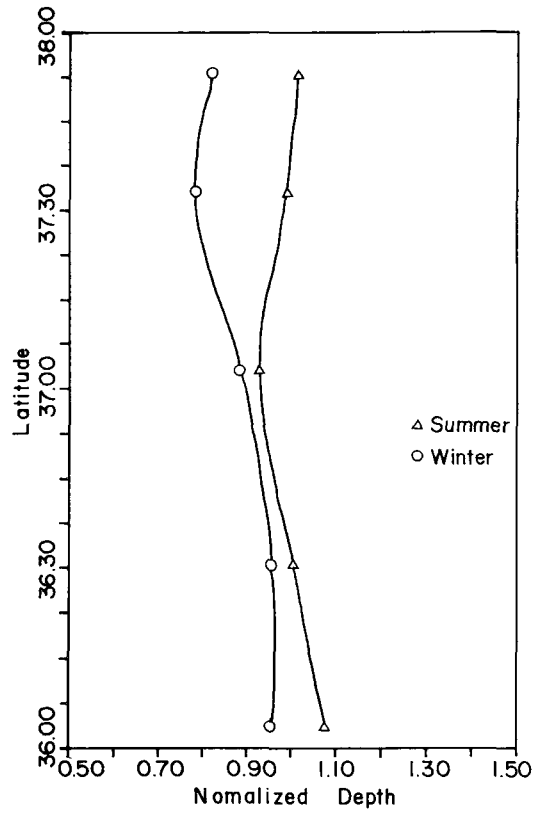

Fig. 7. Seasonal variations of upper layer thickness h^2/hx_0^2.

Discussion

The wind field obtained from the FRDA serial observations and later modified (amplified) in wind speed based on the buoy No. 6 data was confined to a small sector of the whole Sea of Japan. Since, for the present simplified two layer model, the sign and the magnitude of $\frac{\partial \tau}{\partial y}$ is a important factor to determine the local thickness of the upper layer (Eq. 17), further northern or southern extent of the τ distribution is desirable but not an essential factor for the present study. Rather zonal variations over the whole Sea of Japan, if it exists, may be necessary to see an east-west distribution of the upper-layer thickness.

The wind stress distribution that has been used for the numerical investigations of the Tsushima Current (Yoon, 1982. Sekine, 1987) was such that wind stress becomes stronger northward during the winter monsoon and weaker but opposite in direction during the spring-summer season. Thus an anticyclonic and a cyclonic wind stress imposed on the sea surface during the winter and spring-summer season respectively. With such wind stress, a gradual thinning of the upper-layer depth northward over the whole Sea of Japan can be easily expected (Sekine, 1987).

Based on the equation (15), Sverdrup meridional transport relation, and the pure Ekman drift due to wind stress summer and winter transport have been calculated (Fig. 9). February and March and treated as winter season when the volume transport through the strait is minimum and August and October correspond to the summer with the maximum transport by the Tsushima Current (Fig. 10). It is interesting to note that during the months of maxi-

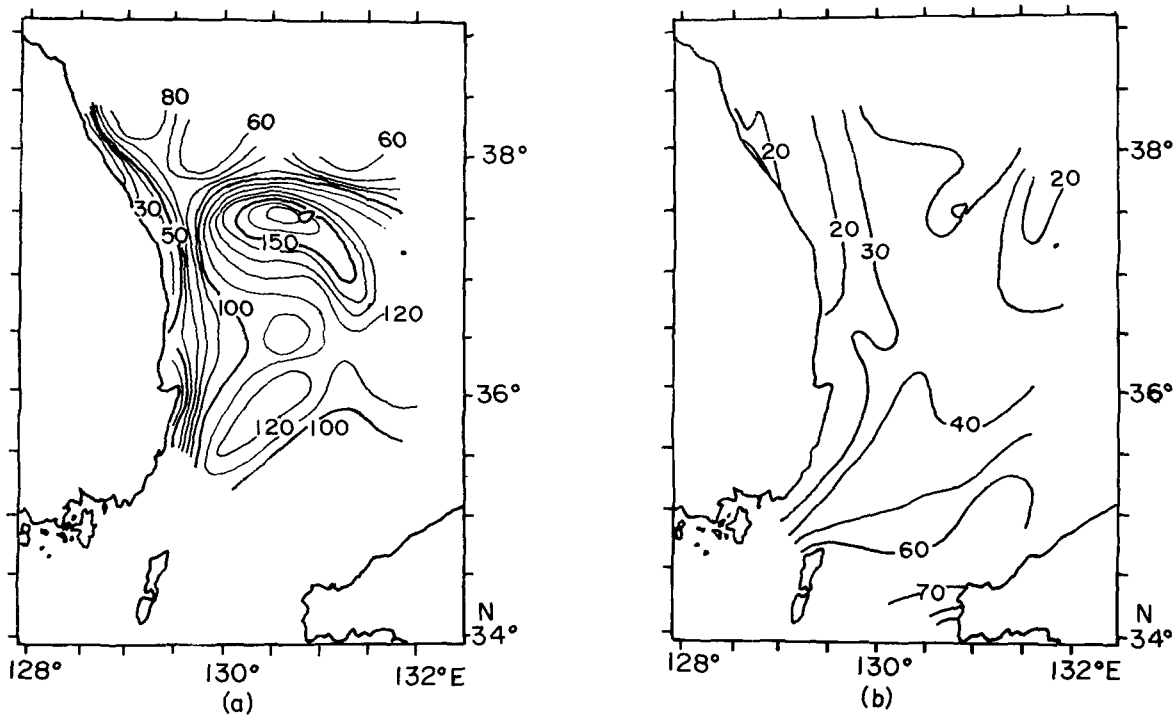

Fig. 8. Mixed layer depth (a) February, and (b) October.

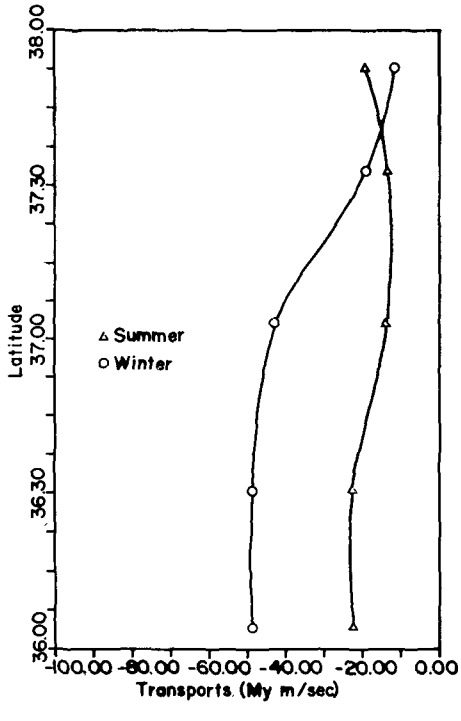

Fig. 9. Wind-driven southward transport for summer and winter season.

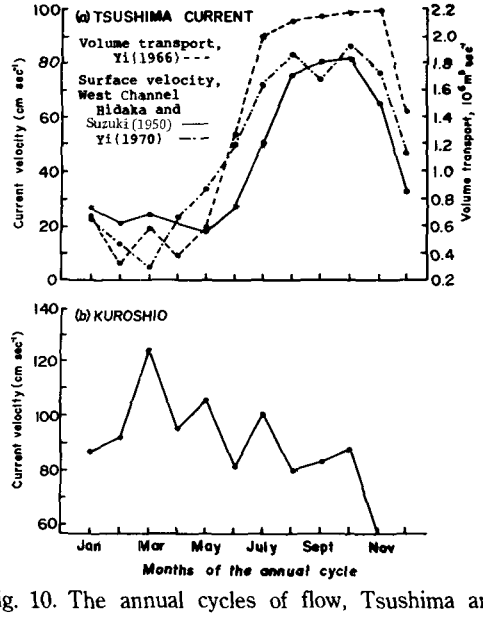

Fig. 10. The annual cycles of flow, Tsushima and Kuroshio : (a) mean monthly surface current velocity (west channel) and the northward volume transport, both channel, line U of the Tsushima Current (b) mean monthly surface velocity of the Kuroshio (Huh, 1982).

mum northward transport through the strait the wind-driven southward flow is much less than the flow of the winter season (Fig. 9). If the Tsushima Current is a flow of water derived directly from the Kuroshio, then the fluctuation of the Kuroshio with some time lag will govern the seasonal variations of the volume transport through the Korea Strait. The time lag based on the speed of surface current at the axis of the Kuroshio near northwest to the Ryukyu Island (Guan, 1981) is about ten days that is far shorter than the one appears on the Fig. 10, which is about six months.

Therefore it could be speculated that the Tsushima Current and its seasonal variation is influenced by the strength of southerly flow driven by the wind stress over the East Sea of Korea. This is not a new idea, since under the distinct summer and winter monsoon with their wind stress pattern the Ekman drift will be opposite to the northward flow through the strait (Huh, 1982). This study just shows the qualitative picture that explaine the seasonal behavior of the meridional transport opposite to the Tsushima Current.

The present model only deals with the interior dynamics of the ocean in that sharp east-west variations of the interface along the east coast of Korea can not be explained. The equation (17), however, describes the tendency of the shallow thermocline westward of the East Sea of Korea provided that the terms in the square braket are positive.

Finally it should be pointed out that over the study area the zonal winds are dominant over the meridional components all year around despite the synoptic fronts passing through the peninsular during the monsoon season. This arises strongly the possible disturbances, like lee waves, when the zonal winds cross over the mountain barriers of north-south direction.

Conclusion

The wind stress distribution over the East Sea of Korea was obtained from the shipboard observations of FRDA along the serial observation lines, These monthly and annual mean wind stress distributions were put into the simplified interface model which describes the latitudinal variations of the upper-layer thickness as function of the curl of the wind stress.

The observed variations of the suface, zonally averaged winds indeed caused the upper-layer flow convergent and divergent at the latitudes that produced a zone of thick upper-layer or a deep permanent thermocline and the shollower depth with divergence. Thus, the wind field contributes positively to maintain the almost time-independent distribution of the interface of "saddle like" feature in north-south direction over the study area.

Futhermore, the wind-driven meridional transport is seasonally changing such that the winter-time transport is twice greater than that of summer-time and it could inhibit the northward flow of the Tsushima Current across the Korea Strait to minimize the resultant volume transprt during the winter season.

For the present study, instead of the overall distribution of the wind stress, zonal distribution of wind is preferable to see the logitudinal variations of the upper-layer thickness because of the dominance of the zonal compoent of the winds that could be affected after crossing over the mountain. In this simplified two-layer model the observed wind stress and its rotational force provided the mechanism that can be used to explain the phenomena dealing with the permanent thermocline and the seasonal fluctuations of the Tsushima Current.

References

Byun, S. K. and S. D. Chang. 1984. Two branches of Tsushima Warm Current in the western channel of the Korea Strait. J. Oceanol. Soc. Korea 19, 200~216.

Guan, B. X. 1981. Some results from the study of the variation of the Kuroshio in the East China Sea, in Collected Oceanic Works. People's Republic of China 4, 1~14.

Hong, C. H. and K. D. Cho. 1983. The northern boundary of the Tsushima Current and its fluctuations. J. Oceanol. Soc. Korea 18, 1~9.

Huh, O. K. 1982. Spring season stagnation of the Tsushima Current and its separation from the Kuroshio : Satellite evidence. J. of Geophy. Res. 87. C12, 9687~9693.

Kang, Y. O. 1985. Seasonal variation of heat content in the neighbouring seas of Korea. J. Oceanol. Soc. Korea 20(3), 1~5.

Lee, J. C. and C. Whang. 1987. One the seasonal variations of surface current in the Eastern Sea of Korea. J. Oceanol. Soc. Korea 16, 1~11.

Mitta, T. and Y. Ogawa. 1984. Tsushima currents measured with current meters and drifters. Ocean Hydrodynamics of the Japan and East China Seas. Elsevier. 67~76.

National Federation of Fisheries Cooperatives. 1977. Oceanographic environments and fisheries resources off the east coast of Korea.

Yi, S. U. 1966. Seasonal and secular variation of the water column transport across the Korea Strait. J. Oceanol. Soc. Korea 1, 7~13.

Sekine, Y. 1986. Wind-driven circulation in the Japan Sea and its influence on the branching of the Tsushima Current. Progress in Oceanography. Pergamon Press. 17, 297~312.

Veronis, G. 1973. Model of World Ocean Circulation : I. Wind-driven, two-layer. J. Mar. Res. 31, 228~288.

Yoon, J. H. 1982. Numerical Experiment on the Circulation in the Japan Sea. Part I, II and III. J. Oceanogr. Soc. Japan 38, 43~51, 81~94, 125~130.

Received September 9, 1988
Accepted October 20, 1988